electronics

MDPI

Article

Simulation and Characteristics Analysis of Multiple Wind Generators in Large-Scale Wind Farms Based on Simplified Model

Jing Wang [1] and Guopeng Zhao [2,*]

[1] School of Mechanical Electronic and Information Engineering, China University of Mining and Technology-Beijing, Beijing 100083, China; zqt1800404077g@student.cumtb.edu.cn

[2] School of Electrical and Electronic Engineering, North China Electric Power University, Beijing 102206, China

* Correspondence: zhaoguopeng@ncepu.edu.cn

Received: 8 November 2020; Accepted: 23 November 2020; Published: 25 November 2020

Abstract: In the view of the high complexity and a large amount of data of the electromagnetic transient model for the single wind generator, it is difficult to realize the multi-unit simulation modeling of large-scale wind farms by power system simulation software. In this paper, the simplified models of single direct drive and doubly-fed wind generator system are proposed, respectively. In order to study the output characteristics of the wind generator system, the components with small inertia constant in the electromagnetic transient model are neglected, and the shafting model, the converter model, and the control loops are simplified and reduced, respectively. Based on the study of the single electromagnetic transient model of wind generators, the simplified simulation models are built by the PSCAD (Power Systems Computer Aided Design) simulation platform, which are carried out under the conditions of constant wind speed, step wind speed, and fault. The output characteristics of the simplified models under different working conditions are compared in detail models. The simulation results show that, within the allowable calculation accuracy range, the dynamic response curves of the single simplified model and the electromagnetic transient model are consistent. The simulation speed can be significantly improved, the time consumption can be reduced, and the simulation speed can be increased more obviously when the number of simulation models increases. Therefore, it can be applied to the simulation research of multi-wind generators in large-scale wind farms.

Keywords: direct drive; doubly-fed; converter; electromagnetic transient model; simplified model

1. Introduction

As energy and environmental issues become more severe, wind energy has been widely used in power systems due to its technological and cost advantages. Electromagnetic transient simulation is an important tool for studying the operation of the grid power system [1]. At present, electromagnetic transient models are the main research objects for wind power generation systems, including wind turbines, drive shafts, generators, converters, and control systems [2,3]. For the research of a single wind generator, one detailed electromagnetic transient simulation model can be easily established to comprehensively observe its response characteristics [4]. However, a wind farm usually includes a dozen to hundreds of wind generators, with smaller simulation step size (microsecond level) of traditional electromagnetic transient simulation calculations, the calculation speed of simulation is greatly reduced, and even becomes unacceptable. A large number of electromagnetic transient models will make the power system simulation model extremely complicated, which is not suitable for large-scale wind farm research. Therefore, it is urgent to find a new and more efficient method to solve this problem.

In [5,6], wind generation units were grouped according to the wind speed range of the power characteristic curve of the wind turbine. With the isolation of the full-power converter, the selection of clustering indicators for permanent magnet direct-drive wind turbines became more complicated, making the accuracy of the equivalent model not high. Although the clustering method could simulate the output characteristics of a large-scale wind farm, it sacrificed the characteristics of a single wind generation unit. In [7], a wind farm equivalent model that only kept constant power current sources and grid-side converters was established. However, for large-scale wind farms, this method had relatively large errors. In [8,9], although it considered the low voltage ride-through characteristics of permanent magnet direct-drive wind generators, wind speed was still selected as the clustering index. The clustering results were difficult to accurately reflect the difference in the operating status of the unit during the low voltage ride-through period, and the accuracy of the equivalent model was lower. In [10], the wind turbines in a wind farm were divided into different sections, and equivalent models were built by establishing wind turbines in different sections. Although the simulation efficiency was improved, the characteristics of a single wind power system were reduced. In [11], two reference dimensions of active power and terminal voltage of doubly-fed wind turbines were added based on wind speed modeling to reflect the state of the pitch angle of doubly-fed wind turbines. However, the application of the wind farm was not sufficient, which needed further research. In [12,13], the researchers put forward several reference factors and basis for wind farm clustering based on the wind farm cluster and its scale effect. But it sacrificed a certain degree of precision. In [14], the researchers selected the speed index when the doubly-fed wind turbine failed, and many other indicators that can reflect the operating state of the doubly-fed wind turbine, to construct a state variable matrix to achieve the grouping of the units. However, the accuracy after being grouped needed to be improved. In [15,16], with many studies on the equivalence of the collector line parameters of wind farms, the voltage difference method and equal power loss method were proposed, based on capacity weighting. However, the weighting method still had inevitable errors. In [17], a detailed converter model and a simplified converter model were established for comparative research. For transient characteristics, if the disturbance is small, the error caused by the simplified model can be ignored; if the disturbance is large, the simplified model may draw wrong conclusions. In [18], a simplified three-order dynamic model of a doubly-fed generator was established with the biaxial components of the rotor excitation voltage and the mechanical torque input by the generator as the control variables. This model could describe the dynamic characteristics of the generator more accurately. But its order was relatively higher, so it could be further simplified. In [19], a practical equivalent method for wind farms based on active power response was proposed. The fault response characteristics of the grid connection points before and after the equivalent value were analyzed. However, there were fewer observable parameters for the wind generator system.

According to the needs of studying the output characteristics of wind generators, in this paper, the simplified models of direct drive and doubly-fed wind generators are proposed, which are built based on the mathematical models. By mathematical method simplification, simplified control loops and system parameters can be obtained. By simplification of a single unit and then application to a multi-unit system, the simulation efficiency can be significantly improved without sacrificing the characteristics and accuracy of the single unit. Moreover, there is no need to change the simulation software algorithm while reducing the dependence on computer performance. In the simplified models proposed in this paper, the shaft model, converter model, and control system model are simplified and the smaller inertia constant in the electromagnetic transient model is ignored. The simplified models can maintain high consistency with the dynamic curve of the electromagnetic transient model under constant, step wind speed and fault conditions, which significantly improve the simulation speed and shorten the time-consumption. The verification shows that the application of the simplified models proposed in this paper to the simulation research of large-scale multi-unit wind farms also has good results. Therefore, they can be applied to large-scale multi-unit wind farms simulation research.

2. Model Simplification Method

2.1. Simplification of Sub-Models

2.1.1. Simplification of Drive Shaft Model

For wind power generation systems of different grid-connected types, the shafting model has a unified structure, including three masses: wind turbine mass, gearbox mass, and generator mass (direct drive wind power generation system has no gearbox mass) [20]. The inertia of the gearbox is smaller compared with that of the fan and generator, which can be ignored. With neglection of the damping coefficient and rigidity coefficient of the transmission shaft, the rotation equation of the traditional simple mass model is obtained:

$$T_{\mathrm{m}} - T_{\mathrm{e}} = J\frac{d\omega}{dt}, \tag{1}$$

where ω is the motor mechanical speed, T_{m} is the mechanical torque, T_{e} is the electromagnetic torque, J is the moment of inertia.

2.1.2. Simplification of Converter Model

With the very high switching frequency of the power electronic devices in the detailed model, the model simulation time-consumption is lengthened. If only the external characteristics of the wind turbine are studied, there is no need to pay attention to the on-off process inside of the converter. Therefore, the equivalent processing of this part can simplify the model greatly.

The simplified electromagnetic transient model usually replaces the converter with a controllable voltage source, ignoring the dynamic process inside the converters. The actual value of the control signal is considered as equal to the reference value, and the input signal of the controllable voltage source is considered as the PWM (Pulse Width Modulation) space vector modulation reference to the voltage command [20]. The simplified electromagnetic transient model not only guarantees the model simulation accuracy, it improves the model simulation speed. However, it still retains most of the remaining structures of the wind generation system, which still has shortcomings to the simulation of large-scale multi-unit wind farms, so it can be further simplified. The replacement of the converter model by a controllable current source, which is an electromechanical transient model, will improve the simplification of the model more significantly.

2.2. Simplification of the Model of a Single Wind Generator

2.2.1. Simplification of a Single Direct Drive Fan Model

The permanent magnet synchronous wind power system installs a full-power converter between the stator winding and the grid to convert the variable-frequency and variable-voltage alternating current output by the generator into a DC voltage, and then it is inverted into an alternating current whose frequency, amplitude, and phase are consistent with the grid and merges it into the grid to achieve variable speed and constant frequency.

The direct drive wind generator unit is mainly composed of a wind turbine, a drive shaft, a permanent magnet synchronous generator (PMSG), a converter and a control system [21,22], whose structure is shown in Figure 1. In the two-phase synchronous rotating coordinate system, the mathematical model of PMSG is obtained:

$$\begin{cases} u_{\mathrm{d}} = R_{\mathrm{s}} i_{\mathrm{d}} - p\omega L_{\mathrm{q}} i_{\mathrm{q}} + L_{\mathrm{d}} \frac{di_{\mathrm{d}}}{dt} \\ u_{\mathrm{q}} = R_{\mathrm{s}} i_{\mathrm{q}} - p\omega L_{\mathrm{d}} i_{\mathrm{d}} + L_{\mathrm{q}} \frac{di_{\mathrm{q}}}{dt} + p\omega\psi_{\mathrm{f}} \\ T_{\mathrm{e}} = \frac{3}{2} p\left[\psi_{\mathrm{f}} i_{\mathrm{q}} + \left(L_{\mathrm{d}} - L_{\mathrm{q}}\right) i_{\mathrm{d}} i_{\mathrm{q}}\right] \end{cases}, \tag{2}$$

where i_{d}, i_{q}, u_{d}, u_{q} are stator d, q axis current and voltage, respectively; R_{s} is stator resistance; p is the number of generator rotor pole pairs; ψ_{f} is the rotor permanent magnet flux linkage; ω is the generator rotor speed.

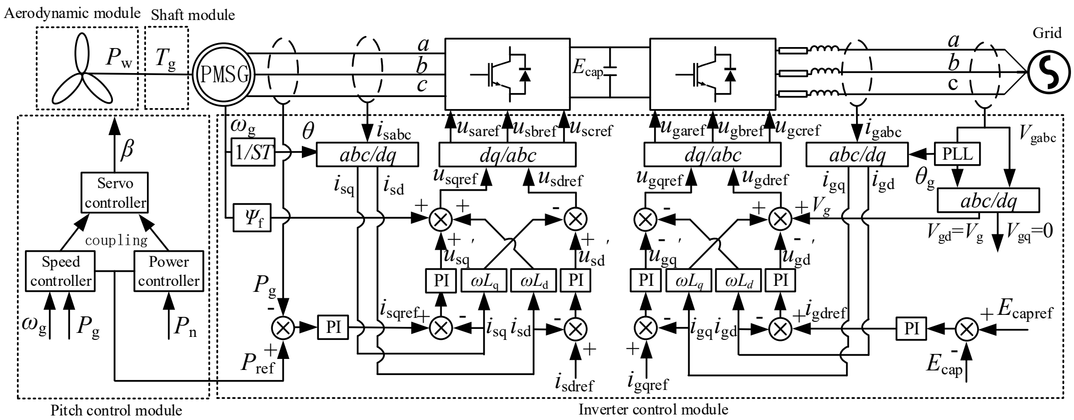

Figure 1. Direct-drive fan structure and its control.

Since the direct drive wind generator does not have a gearbox, $\omega = \omega_{\mathrm{g}}$ (ω_{g} is the generator rotor speed). The following equations can be obtained:

$$\begin{cases} T_{\mathrm{m}} = \frac{P_{\mathrm{m}}}{\omega} \\ T_{\mathrm{e}} = \frac{P}{\omega} \end{cases}. \tag{3}$$

Additionally, the generator side power is:

$$\begin{cases} P = \frac{3}{2}\left(u_{\mathrm{d}} i_{\mathrm{d}} + u_{\mathrm{q}} i_{\mathrm{q}}\right) \\ Q = \frac{3}{2}\left(u_{\mathrm{q}} i_{\mathrm{d}} - u_{\mathrm{d}} i_{\mathrm{q}}\right) \end{cases}, \tag{4}$$

where P_{m} is the mechanical power output by the wind turbine; P is the electromagnetic active power output by the generator; Q is the electromagnetic reactive power output by the generator.

The generator-side converter uses the generator rotor flux vector control method, which is usually $i_{\mathrm{sd}} = 0$ control [23], to control the electromagnetic torque output by the generator and then control the generator speed to achieve the purpose of maximum power point tracking (MPPT). The grid-side converter inverts DC power into AC power. The converter adopts double closed loop control, the outer loop is the power loop, and the inner loop is the current loop.

The electromagnetic time constant of the inner current loop is much smaller than the electromechanical time constant of the outer loop, and the response speed of the inner loop is faster than that of the outer loop. Therefore, in the simplified model, the dynamic process of the current inner loop of the converter is ignored, and the input value of the inner loop is considered equal to output value. The generator output power value P is compared with the reference signal P_{ref}, and the control command i_{sqref} of the current inner loop is obtained by the PI regulator, which is considered equivalent to the current inner loop output value i_{sq}, and $i_{\mathrm{sd}} = 0$ is brought into the control system. The following equations can be obtained:

$$\begin{cases} u_{\mathrm{q}} = R_{\mathrm{s}} i_{\mathrm{q}} + L_{\mathrm{q}} \frac{di_{\mathrm{q}}}{dt} + p\omega\psi_{\mathrm{f}} \\ P = \frac{3}{2} \mathrm{u}_{\mathrm{q}} i_{\mathrm{q}} \end{cases}. \tag{5}$$

The simplified model of the direct drive wind generator is shown in Figure 2. The fan module calculates the mechanical torque T_{m} through the wind speed V_{w} and the rotor speed ω, and then it is brought into the rotor motion equation. The MPPT model calculates the power reference value P_{ref} through the wind speed V_{w} and the rotor speed ω. After the reference value P_{ref} is compared with the actual value P, the inner loop current reference value i_{sqref} is obtained through the PI controller. Since the inner loop is simplified, its output is equal to its input. After the current value i_{sq}, i_{sd} brought into the stator voltage equations, the stator voltages U_{sabc} are obtained through coordinate transformation. With the active power value P and grid voltage U_{gabc}, the grid current value i_{gd}, i_{gq} are calculated. Then, the reference command value of the controlled current source is obtained through coordinate transformation.

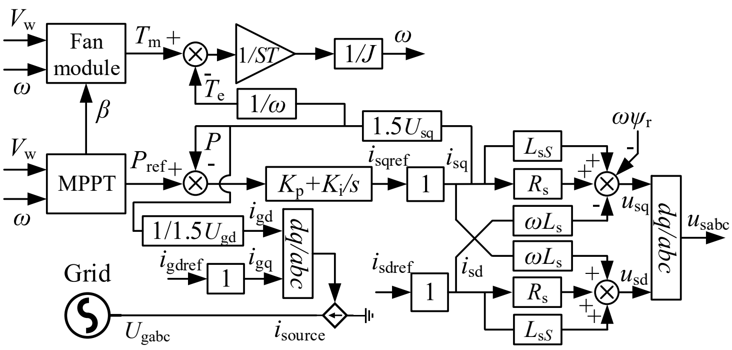

Figure 2. Simplified model of the direct drive wind generator.

2.2.2. Simplification of a Single Doubly-Fed Wind Generator Model

The doubly-fed wind generator unit is mainly composed of doubly-fed induction generator (DFIG), machine-side converter, grid-side converter and its control system [24]. The wind turbine is connected to the generator after speed-increasing by gears, and a converter is used to realize the two-way flow of power with the grid. The structure of the doubly-fed wind generator is shown in Figure 3.

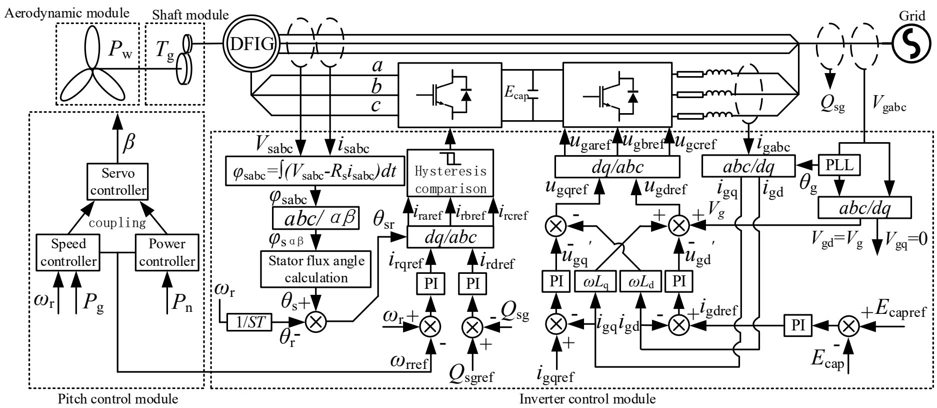

Figure 3. Doubly-fed wind generator structure and its control.

When the stator flux directional control is adopted [25], the stator flux ψ_{sd} is equal to ψ_{s}, and $\psi_{\mathrm{sq}} = 0$. Since the stator of the doubly-fed generator is directly connected to the grid, the stator voltage amplitude U_{s} is a constant, that is, the grid voltage, and the equation $p\omega\psi_{\mathrm{s}} = U_{\mathrm{s}}$ can be obtained. The electromagnetic torque and the stator flux equation of the generator are as follows:

$$\left\{ \begin{array}{lcl} T_{\mathrm{e}} & = & \psi_{\mathrm{rd}} i_{\mathrm{rd}} - \psi_{\mathrm{rq}} i_{\mathrm{rq}} \\ \psi_{\mathrm{sq}} & = & -L_{\mathrm{s}} i_{\mathrm{sq}} + L_{\mathrm{m}} i_{\mathrm{rq}} \\ \psi_{\mathrm{sd}} & = & -L_{\mathrm{s}} i_{\mathrm{sd}} + L_{\mathrm{m}} i_{\mathrm{rd}} \end{array} \right. . \tag{6}$$

where L_s and L_m are the self-inductance of the stator and the mutual inductance between the stator and rotor, respectively. The value of electromagnetic torque T_e can be obtained, $T_e = \frac{L_m U_s}{L_s p \omega} i_{rq}$.

The converter adopts double closed-loop control, the outer ring is the rotating speed loop, and the inner ring is the current loop. Similarly, in this simplified model, the dynamic process of the current inner loop of the converter is ignored, and the input of the inner loop is considered equal to the output. The speed ω is compared with the reference signal ω_{ref}, and the control command i_{qref} of the current inner loop is obtained by the PI regulator, which is considered equivalent to the output value of the current inner loop. Then, the electromagnetic torque T_e is calculated, which is brought into the motion equation of the drive shaft system to obtain the speed ω to feedback. The simplified model of the doubly-fed wind generator is shown in Figure 4.

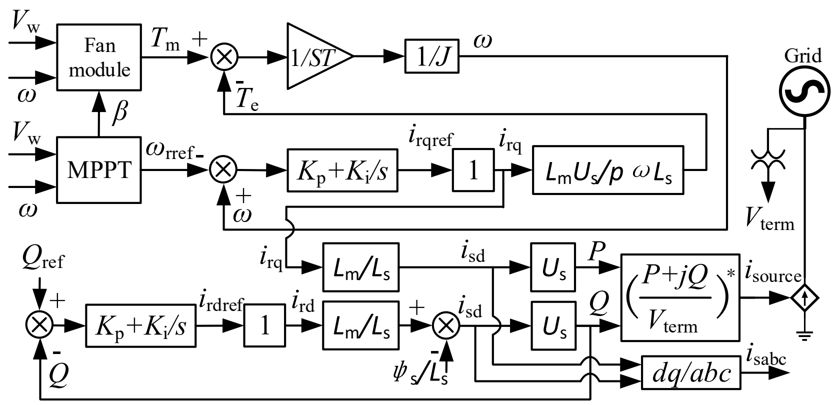

Figure 4. Simplified model of the doubly-fed wind generator.

The fan module calculates the mechanical torque T_m through the wind speed V_w and the rotor speed ω, and then it is brought into the rotor motion equation. The MPPT model calculates the rotor speed reference value ω_{ref} through the wind speed V_w and the rotor speed ω. After the reference value ω_{ref} is compared with the actual value ω, the inner loop current reference value i_{rqref} is obtained through the PI controller. Since the inner loop is simplified, its output is equal to its input. After current value i_{rq}, i_{rd} brought into the stator current equations, the stator currents i_{sabc} are obtained through coordinate transformation. After current value i_{rq}, i_{rd} brought into the power equations, the stator active and reactive power P, Q are obtained through coordinate transformation. With the active and reactive power P, Q, and grid voltage V_{term}, and then the reference command value of the controlled current source is obtained.

3. Simplified Model and Simulation of Wind Generator

3.1. Simplified Model Parameters of Direct-Drive, Doubly-Fed Wind Generator

In order to verify the correctness of the simplified model of a single direct-drive and doubly-fed wind generator based on PSCAD, simulation analysis was carried out under three conditions of constant wind speed, step wind speed, and fault. The model parameters are as shown in Table 1.

Table 1. Wind generators parameters.

Parameters of PMSG		Parameters of DFIG	
Rated capacity	0.5 MVA	Rated capacity	0.5 MVA
Rated voltage	0.69 kV	Rated voltage	0.69 kV
Rated frequency	20 Hz	Rated frequency	50 Hz
D axis inductance	0.5 (pu)	Stator resistance	0.005 (pu)
Q axis inductance	0.5 (pu)	Stator inductance	0.1 (pu)
Magnetic strength	1.0 (pu)	Rotor inductance	0.11 (pu)

3.2. Simulation Results of a Single Wind Generator under Constant Wind Speed Conditions

The simulation step sizes are set to 20,100 µs, respectively. The simulation duration is 20 s, and the constant wind speed is set to 9 m/s. The simulation time-consuming and accuracy comparison results of the detailed model and simplified model built on the PSCAD are shown in Tables 2 and 3, respectively.

Table 2. Model simulation time-consuming comparison results.

Type	Number	Simulation Step Size	Time-Consuming/s		Time-Consuming Ratio
			Detailed Model	Simplified Model	
Direct drive wind generator	1	20 100	530 142	12 11	44.2 12.9
	5	20 100	2430 547	24 20	101.3 27.4
Doubly-fed wind generator	1	20 100	493 131	13 12	37.9 10.9
	5	20 100	2256 522	26 24	86.8 21.75

Table 3. Model simulation accuracy comparison results.

Type		Rotating Speed	Grid Current	Output Power of Generator
		r/min	kA	MW
Direct drive	Detailed model Simplified model	94.2 94.4	0.295 0.310	0.386 0.387
Error	%	0.2	5.1	0.3
Doubly-fed	Detailed model Simplified model	1220.5 1220.5	0.296 0.311	0.387 0.388
Error	%	0.0	5.1	0.3

It shows in Table 2 that under the same simulation step size, since the simplified model does not take the on-off process of power electronic devices in the converter into account, the simulation time-consumption is reduced greatly than the detailed model. When the number of wind generators increases, the simulation efficiency increases more significantly. Therefore, when studying large-scale multi-unit wind farms, the simplified models proposed in this paper have a significant effect in shortening the simulation time-consumption and improving the simulation efficiency.

It shows in Table 3 that with the simplified models proposed in this paper, the error does not exceed 10%. The grid current errors of models are relatively large, mainly due to the switching loss of converters in the detailed model, which is ignored in the simplified models. Therefore, the models proposed in this paper obviously keep good consistency with the detailed models within the reasonable accuracy range.

3.3. Simulation Results of a Single Wind Generator under Step Wind Speed Condition

In order to verify the effectiveness of the simplified model in analyzing the dynamic process, the two types of wind generator models are run under step wind speed condition. The wind speed is set to step from 8 m/s to 10 m/s at t = 10 s.

3.3.1. Simulation Results of a Single Direct Drive Wind Generator

Since the permanent magnet synchronous wind power generation system adopts the variable-speed constant-frequency control method, the speed of the wind turbine can be adjusted according to the change of wind speed, so will the speed of the PMSG accordingly. When the rotation speed of the

PMSG changes, the voltage and frequency generated at the stator will also change, so will the output power of the generator accordingly. As shown in the Figure 5, when the wind speed stepped from 8 to 10 m/s at t = 10 s.

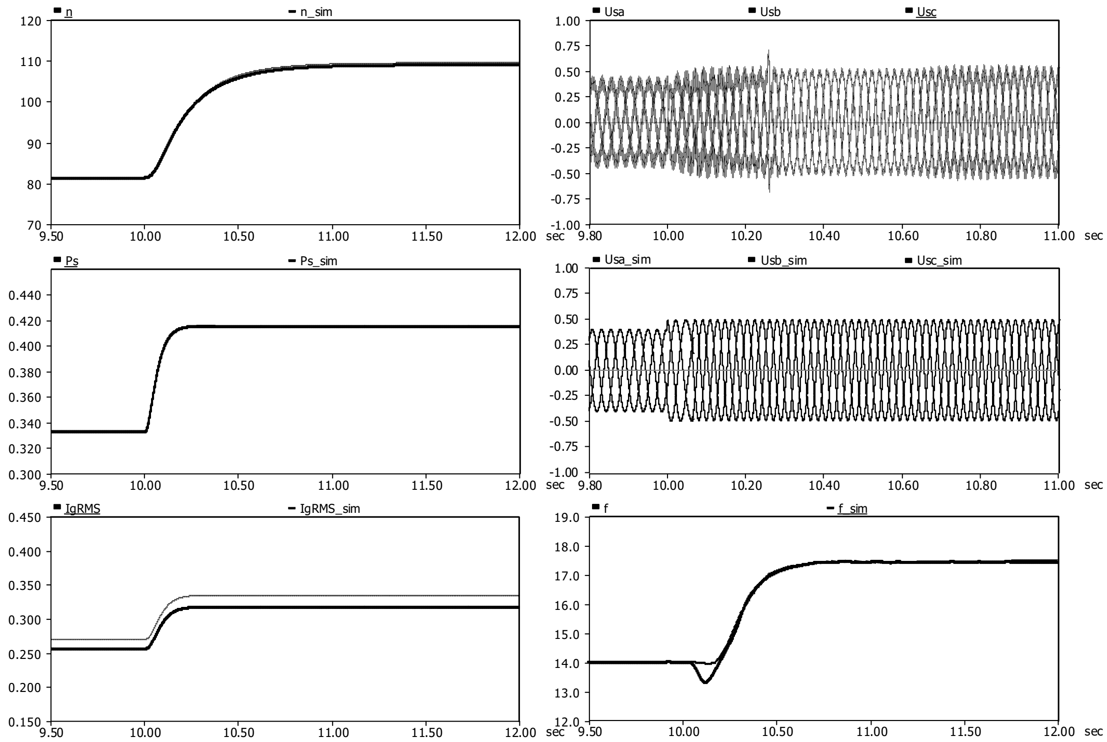

Figure 5. Comparison of characteristics under step wind speed conditions (direct drive wind generator).

In the detailed model, the PMSG speed n gradually increased from 81.2 r/min, and stabilized to 109.0 r/min at t = 11.5 s; in the simplified model, the PMSG speed $n_{\_sim}$ increased from 81.1 r/min (error: 0.1%), gradually increased and stabilized to 109.5 r/min (error: 0.5%) at t = 11.5 s.

In the detailed model, the output power P_s of the PMSG gradually increased from 0.333 MW, and stabilized to 0.415 MW at t = 10.5 s; in the simplified model, the output power P_{s_sim} of the PMSG increased from 0.333 MW (error: 0.0%), gradually increased and stabilized to 0.415 MW (error: 0.0%) at t = 10.5 s.

In the detailed model, the value of the grid-connected current I_{gRMS} of the direct drive wind generator gradually increased from 0.255 kA, and stabilized to 0.317 kA at t = 10.5 s; in the simplified model, the value of the grid-connected current I_{gRMS_sim} of the direct drive wind generator increased from 0.270 kA (error: 5.9%), gradually increased and stabilized to 0.333 kA (error: 5.0%) at t = 10.5 s.

In the detailed model, the amplitude of the PMSG stator voltage U_{sabc} gradually increased from 0.40 kV and stabilized to 0.49 kV at t = 11.0 s, the voltage frequency f gradually increased from 14.1 Hz, and stabilized to 17.5 Hz at t = 11.0 s; In the simplified model, the amplitude of the PMSG stator voltage U_{sabc_sim} gradually increased from 0.40 kV (error: 0.0%), and stabilized to 0.49 kV (error: 0.0%) at t = 11.0 s, and the voltage frequency $f_{\_sim}$ increased from 14.0 Hz (error: 0.7%) gradually increased, and stabilized to 17.5 Hz at t = 11.0 s (error: 0.0%).

The relatively large error between grid-connected current I_{gRMS} and I_{gRMS_sim} is mainly due to the installation of a full-power converter between the PMSG and the grid, so there is switching loss in the detailed model, which is ignored in the simplified model. The error is within 10%.

In conclusion, when the wind speed changes, the simplified direct-drive wind generator model can achieve the purpose of maximum power point tracking, while also maintaining good consistency with the dynamic and steady state characteristics of the detailed model.

3.3.2. Simulation Results of a Single Doubly-Fed Wind Generator

Since the doubly-fed wind generation system adopts the variable-speed constant-frequency control method, the speed of the wind turbine can be adjusted according to the change of wind speed, so will the speed of the DFIG will also change accordingly. When the rotor speed of the DFIG changes, the stator current frequency is kept consistent with the grid frequency by adjusting the rotor current frequency, that is, 50 Hz. Further, the output power of the generator will change accordingly. As shown in the Figure 6, when the wind speed stepped from 8 to 10 m/s at t = 10 s.

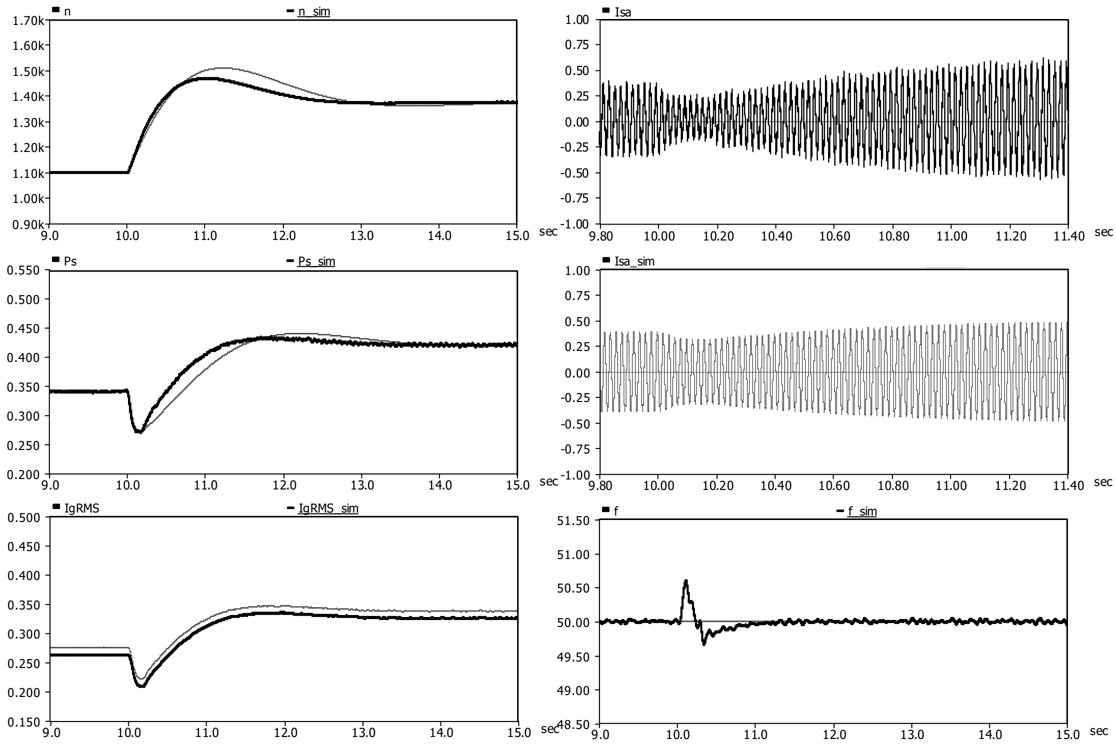

Figure 6. Comparison of characteristics under step wind speed conditions (doubly-fed wind generator).

In the detailed model, the DFIG rotor speed n gradually increased from 1099 r/min, and stabilized to 1375 r/min at t = 14 s; in the simplified model, the DFIG rotor speed $n_{\_sim}$ increased from 1100 r/min (error: 0.1%), gradually increased and stabilized to 1375 r/min (error: 0.5%) at t = 14 s.

In the detailed model, the output power P_s of the DFIG gradually increased from 0.340 MW, and stabilized to 0.420 MW at t = 14 s; in the simplified model, the output power P_{s_sim} of the DFIG increased from 0.341 MW (error: 0.3%), gradually increased, and stabilized to 0.421 MW at t = 14 s (error: 0.2%).

In the detailed model, the value of the grid-connected current I_{gRMS} of the doubly-fed wind generator gradually increased from 0.262 kA and stabilized to 0.325 kA at t = 14 s; in the simplified model, the value of grid-connected current I_{gRMS_sim} of the doubly-fed wind generator increased from 0.275 kA (error: 5.0%), gradually increased, and stabilized to 0.336 kA (error: 3.4%) at t = 14 s.

In the detailed model, the amplitude of the stator current I_{sabc} of the DFIG gradually increased from 0.389 kA and stabilized to 0.475 kV at t = 14.0 s. The current frequency f is 50 Hz at steady state, and fluctuated at t = 10.0 s (Δf = 0.5 Hz). In the simplified model, the amplitude of the stator current I_{sabc_sim} of the DFIG gradually increased from 0.390 kV (error: 0.3%) and stabilized to 0.476 kV (error: 0.2%) at t = 14.0 s, the current frequency $f_{\_sim}$ is always maintained at 50.0 Hz (error: 0.0%).

The relatively large error between the grid-connected current I_{gRMS} and I_{gRMS_sim} is mainly due to the installation of a converter between the rotor of the DFIG and the grid, so there is a small amount of slip power, and the error is within 10%.

In conclusion, when the wind speed changes, the doubly-fed wind power generation model can achieve the purpose of maximum power point tracking, while also maintaining good consistency with the characteristics of the detailed model.

3.4. Simulation Results of a Single Wind Generator under Fault Condition

In order to verify the effectiveness of the simplified model of the two types of single wind generator under fault condition, both types of wind power generation units are operated under single-phase ground fault condition on the grid-connected side. The constant wind speed is set to 9 m/s. The rated voltage of the grid is 0.69 kV.

3.4.1. Simulation Results of a Single Direct Drive Wind Generator

As shown in the Figure 7, when a phase A grounding fault occurs at the grid-connected end via a 0.1 Ω resistance at t = 10 s.

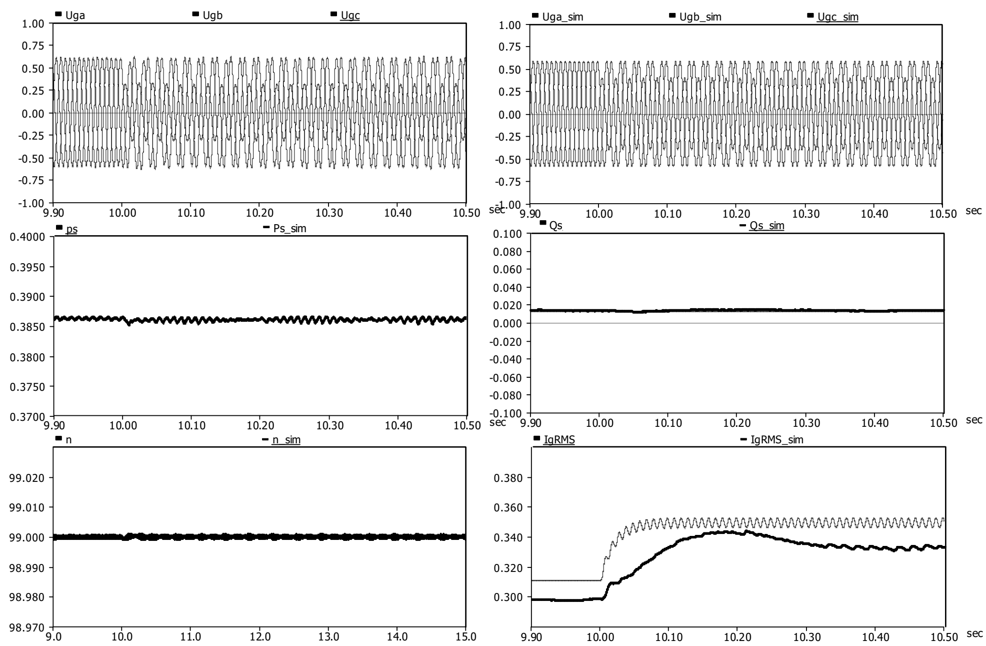

Figure 7. Comparison of characteristics under fault condition (direct drive wind generator).

In the detailed model, the amplitude of phase A voltage U_a of the power grid dropped from 0.584 to 0.392 kV, and the amplitude of phase B, C voltage U_b, U_c remained 0.584 kV without significant change; in the simplified model, the amplitude of phase A voltage U_a of the power grid dropped from 0.585 kV (error: 0.2%) to 0.392 kV (error: 0%), and the B, C phase voltage U_b, U_c amplitude remained 0.585 kV (error: 0.2%) without significant changes.

In the detailed model, the average value of the generator output active power P_s was 0.386 MW without significant change; in the simplified model, the average value of the generator output active power P_{s_sim} was 0.387 MW (error: 0.3%) without significant change.

In the detailed model, the reactive power Q_s of the generator output was 0.014 MVar, whose average value did not change significantly; in the simplified model, the reactive power Q_{s_sim} of the generator output was 0.014 MVar (error: 0.0%), whose average value did not change significantly.

In the detailed model, the rotor speed n of the PMSG maintained at 99.0 r/min all the time, whose average value did not change significantly with only a slight disturbance after 10 s; in the simplified model, the rotor speed of the PMSG $n_{\_sim}$ also maintained 99.0 r/min (error: 0.0%), whose average value did not change significantly.

In the detailed model, the value of the grid-connected current I_{gRMS} of the direct drive wind power generation gradually increased from 0.295 kA, and stabilized to 0.330 kA at t = 10.4 s, containing second-harmonic disturbance; in the simplified model, the value of grid-connected current I_{gRMS_sim} of the direct drive wind power generation gradually increased from 0.310 kA (error: 5.1%), and stabilized to 0.345 kA (error: 4.5%) at t = 10.2 s, containing second-harmonic disturbance.

In conclusion, when a single-phase ground fault occurs on the grid-connected side, the simplified direct-drive wind power model can maintain good consistency with the characteristics of the detailed model.

3.4.2. Simulation Results of a Single Doubly-Fed Wind Generator

As shown in the Figure 8, when a phase A grounding fault occurs at the grid-connected end via a 0.1Ω resistance at t = 10 s.

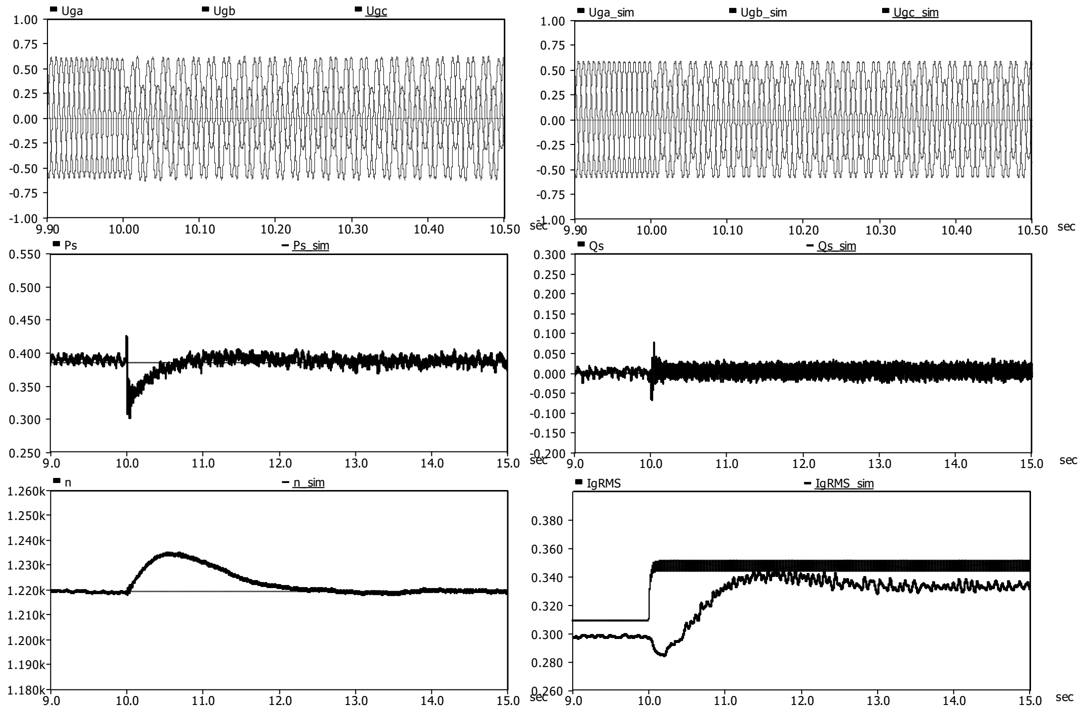

Figure 8. Comparison of characteristics under fault condition (doubly-fed wind generator).

In the detailed model, the amplitude of phase A voltage U_a of the power grid dropped from 0.584 to 0.392 kV, and the amplitude of phase B, C voltage U_b, U_c remained 0.584 kV without significant change; in the simplified model, the amplitude of phase A voltage U_a of the power grid dropped from 0.585 kV (error: 0.2%) to 0.392 kV (error: 0%), the amplitude of phase B, C voltage U_b, U_c remained 0.585 kV (error: 0.2%) without significant changes.

In the detailed model, the generator output active power P_s remained 0.387 MW, whose average value did not change significantly; in the simplified model, the generator output active power P_{s_sim} remained 0.388 MW (error: 0.3%), whose average value did not change significantly.

In the detailed model, the average value the reactive power Q_s of the generator output was 0.01 MVar, which did not change significantly; in the simplified model, the reactive power Q_{s_sim} of the generator output was 0.01 MVar (error: 0.0%), which did not change significantly but with disturbance.

In the detailed model, the rotor speed n of the PMSG changed from 1220.5 r/min after t = 10 s, containing a peak value of 1234.0 r/min fluctuation. In addition, it returned to 1220.5 r/min at t = 14 s. In the simplified model, the rotor speed $n_{\_sim}$ of the PMSG maintained at 1220.5 r/min (error: 0.0%) all the time.

In the detailed model, the value of the grid-connected current I_{gRMS} of the direct drive wind power generation system decreased slightly from 0.295 kA and then gradually increased, which stabilized to 0.331 kA at t = 14 s, containing second-harmonic disturbance; in the simplified model, the value of grid-connected current I_{gRMS_sim} of the direct drive wind power generation system gradually increased from 0.311 kA (error: 5.4%), and stabilized to 0.346 kA (error: 4.5%) at t = 10.2 s, containing second-harmonic disturbance.

The relatively large error between grid-connected current I_{gRMS} and I_{gRMS_sim} is mainly due to the installation of a converter between the rotor side of the DFIG and the grid, so there is a small amount of slip power, and the error is within 10%.

In conclusion, when a single-phase ground fault occurs on the grid-connected side, the simplified doubly-fed wind power model can maintain good consistency with the characteristics of the detailed model.

3.5. Simulation Results of Multi-Unit Hybrid Simplified Model

In order to verify the effectiveness of application of single simplified model to large-scale multi-unit wind farm study, a large-scale multi-unit wind farm was built on the PSCAD software platform. The total installed capacity is 100 units and the total capacity is 50 MW, including 50 direct drive and 50 doubly-fed units. In order to reduce the line loss, every single wind generator is connected to the collector line after being boosted by a 0.69 kv/35 kv transformer. The 100 wind generators are divided into 10 columns, each with 10 units. The unit spacing is 0.15 km, and the row spacing is 0.5 km. The line resistance is 0.2 Ω/km, and the line inductance is 0.002 H/km. Its overall structure is shown in Figure 9. Forty units in rows 1 to 4 are 5 + 5 direct-drive and doubly-fed hybrid units; 30 units in rows 5 to 7 are direct drive units, and 30 units in rows 8 to 10 are doubly-fed units.

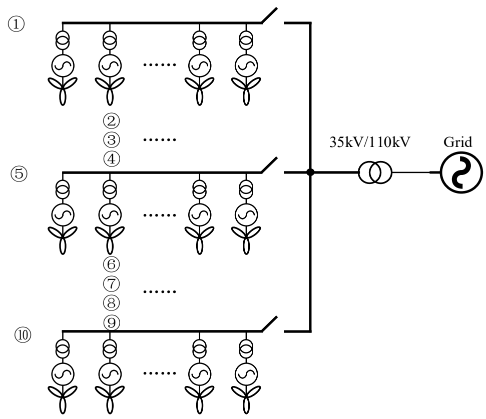

Figure 9. Structure of large-scale wind farm with multiple wind generators.

3.5.1. Simulation Results under Constant Wind Speed Condition

Since the same amount of detailed model data is too large to run on the PSCAD platform, the sum of 50 times the output value of a single detailed model under the same working condition is the expected value. The simulation step size is set to 20, 100 µs, respectively. The simulation duration time is 20 s, and the constant wind speed is set to 9 m/s. The simulation time-consuming and accuracy comparison results are shown in Tables 4 and 5.

Table 4. Results of multi-unit hybrid simplified model simulation time-consuming.

Type	Simulation Step Size	Time Consuming
50 PMSG and 50 DFIG	20	1617
	100	351

Table 5. Comparison results of multi-unit hybrid model simulation accuracy.

Object	Parameters	Actual Value	Expected Value	Error
No. ①	Grid-connected current/kA	0.061	0.058	5.2%
5 + 5	Generator output power/MW	3.874	3.865	0.1%
hybrid units	Grid-connected power/MW	3.741	3.546	5.2%
No. ⑤	Grid-connected current/kA	0.061	0.058	5.2%
10	Generator output power/MW	3.870	3.860	0.3%
Direct drive	Grid-connected power/MW	3.711	3.529	5.2%
No. ⑧	Grid-connected current/kA	0.061	0.058	5.1%
10	Generator output power/MW	3.880	3.870	0.3%
Doubly-fed	Grid-connected power/MW	3.720	3.529	5.2%
① to ⑩	Grid-connected current/kA	0.613	0.583	5.1%
50 + 50	Generator output power/MW	38.750	38.650	0.3%
hybrid units	Grid-connected power/MW	37.148	35.321	5.2%

In Table 4, it shows that the simplified model has a significant effect on shortening the time-consumption. Under the condition that the simulation step size is 20 µs and the simulation duration time is 20 s, the time-consumption (1617 s) of 100 hybrid simplified models is even less than that of the detailed model of 5 doubly-fed wind generators (2256 s). The error between the actual value and the expected value of the simulation results does not exceed 10%. It shows that the single simplified model can still maintain excellent accuracy in large-scale wind farm simulation to study the characteristics of the system.

3.5.2. Simulation Results under Step Wind Speed Condition

When the wind speed is set to step from 8 to 10 m/s at t = 10 s, the output characteristics of wind farm are shown in Figure 10.

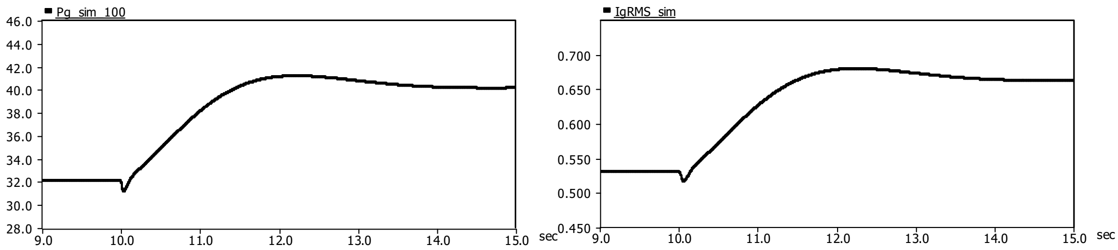

Figure 10. Multi-unit simplified model output characteristic under step wind speed condition.

In the simplified model, at t = 10 s, the grid-connected power $P_{g\_sim\_100}$ of the wind farm gradually increased from 32.138 MW. The line loss $\Delta P = P_{s\_sim\_100} - P_{g\_sim\_100} = 0.333 * 50 + 0.341 * 50 - 32.138 = 1.562$ MW. Assume its expected value with the same line loss: $P_{g\_100} = P_g - \Delta P = 1.731 * 0.69 * (0.255 + 0.262) * 50 = 30.912$ MW, and the error is 4.0%. At t = 14 s, $P_{g\_sim\_100}$ stabilized to 40.051 MW. The line loss $\Delta P = P_{s\_sim\_100} - P_{g\_sim\_100} = 0.415 * 50 + 0.421 * 50 - 40.051 = 1.749$ MW. Assume its expected value with the same line loss: $P_{g\_100} = P_g - \Delta P = 1.731 * 0.69 * (0.317 + 0.325) * 50 = 38.340$ MW, and the error is 4.5%.

In the simplified model, the value of the grid-connected current I_{gRMS} of the wind farm gradually increased from 0.530 kA (Expected value: $P_{g\_100}/(1.731 * U_{rated}) = 30.912/(1.731 * 35) = 0.510$ kA, error: 3.9%). It stabilized to 0.664 kA at t = 14 s (Expected value: $P_{g\_100}/(1.731 * U_{rated}) = 38.340/(1.731 * 35) = 0.633$ kA, error: 4.9%)

Although the line loss is considered, the switching loss of the converter and the slip power are ignored in the simplified models, which lead to the error, but the error is also within 10%. It shows that the simplified multi-unit model can also maintain good consistency with the characteristics of the detailed model under step wind speed condition.

3.5.3. Simulation Results under Fault Condition

Single-phase grounding fault occurs on 35 kV bus at t = 10 s. The constant wind speed is 9 m/s. Under fault condition, the characteristic results of the wind farm model are shown in Figure 11.

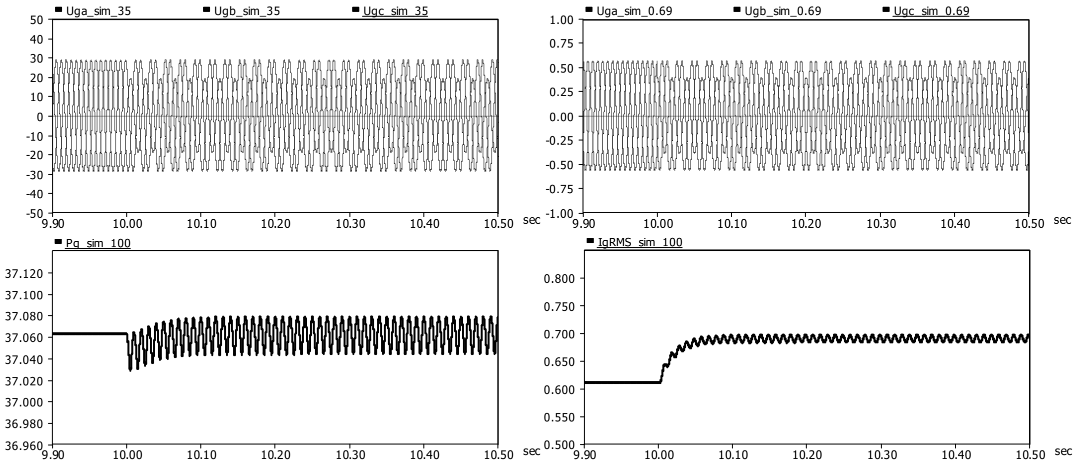

Figure 11. Multi-unit simplified model output characteristic under fault condition.

In the simplified model, for 35 kV bus, the amplitude of phase A voltage U_a of the power grid dropped from 28.62 to 19.1 kV, the amplitude of phase B, C voltage U_b, U_c remained 28.62 kV without significant changes. For 0.69 kV bus, the amplitude of phase A voltage U_a of the power grid dropped from 0.585 to 0.392 kV, the amplitude of phase B, C voltage U_b, U_c remained 0.585 kV without significant changes.

In the simplified model, the steady-state value of wind farm grid-connected power $P_{g\_sim\_100}$ is 37.178 MW, and second-harmonic disturbance began to appear at t = 10 s. In the simplified model, the value of the grid-connected current I_{gRMS} of the wind farm gradually increased from 0.613 kA, and stabilized to 0.690 kA at t = 10.2 s, containing second-harmonic disturbance. It shows that the simplified multi-unit model can also maintain good consistency with the characteristics of the detailed model under single-phase ground fault condition.

4. Conclusions

In the view of the low simulation efficiency of multiple wind generators in large-scale wind farms, the simplified models of single direct drive and doubly-fed wind generator system are proposed in this paper, respectively. Through the simplified models proposed in this paper and its verification, the following conclusions can be obtained:

1. In the simplified models proposed in this paper, the converter model and control system are simplified. The controllable current source and voltage source models are used to replace detailed model converters. Therefore, a large amount of data in detailed models is reduced, which significantly improves the simulation efficiency.
2. The simplified models proposed in this paper are built by mathematical method simplification based on the mathematical models, so there is no need to change the simulation software algorithm and it reduces the dependence on computer performance.
3. The simplified simulation models proposed in this paper not only improve the simulation efficiency, but also maintain good consistency with the simulation results of the detailed model under normal and fault conditions.

4. By simplification of a single unit and then application to a multi-unit system, the characteristics and accuracy of the single unit can be well retained. Therefore, the simplified models have good effects in the research of multiple wind generators in large-scale wind farms.

Author Contributions: Conceptualization, J.W.; methodology, J.W. and G.Z.; software, J.W.; validation, J.W. and G.Z.; formal analysis, J.W. and G.Z.; investigation and resources, J.W. and G.Z.; data curation, J.W. and G.Z.; writing—original draft preparation, J.W. and G.Z.; writing—review and editing, J.W. and G.Z.; supervision, G.Z.; project administration, G.Z. All authors have read and agreed to the published version of the manuscript.

Funding: This research received no external funding.

Conflicts of Interest: The authors declare no conflict of interest.

References

1. Tan, K.; Islam, S. Optimum Control Strategies in Energy Conversion of PMSG Wind Turbine System without Mechanical Sensors. *IEEE Trans. Power Electron.* **2004**, *19*, 392–399. [CrossRef]
2. Muyeen, S.; Al-Durra, A.; Tamura, J. Variable speed wind turbine generator system with current controlled voltage source inverter. *Energy Convers. Manag.* **2011**, *52*, 2688–2694. [CrossRef]
3. Ganjefar, S.; Ghassemi, A.A.; Ahmadi, M.M. Improving efficiency of two-type maximum power point tracking methods of tip-speed ratio and optimum torque in wind turbine system using a quantum neural network. *Energy* **2014**, *67*, 444–453. [CrossRef]
4. Wu, Z.Q.; Jia, W.J. Maximum wind power tracking based on cloud RBF neural network Pitch angle. *Renew. Energy* **2016**, *86*, 446–472. [CrossRef]
5. Fernández, L.M.; Jurado, F.; Saenz, J.R. Aggregated dynamic model for wind farms with doubly fed induction generator wind turbines. *Renew. Energy* **2008**, *33*, 129–140. [CrossRef]
6. Gao, F.; Zhao, D.; Zhou, X.; AN, N. Dynamic equivalent algorithm for wind farm composed of direct-drive wind turbines. *Power Syst. Technol.* **2012**, *36*, 222–227.
7. Conroy, J.; Watson, R. Aggregate modelling of wind farms containing full-converter wind turbine generators with permanent magnet synchronous machines: Transient stability studies. *IET Renew. Power Gener.* **2009**, *3*, 39–52. [CrossRef]
8. Abbes, M.; Allagui, M. An aggregate model of PMSG-based, grid connected wind farm: Investigation of LVRT capabilities. In Proceedings of the International Renewable Energy Congress, Sousse, Tunisia, 24–26 March 2015; pp. 1–6.
9. Qi, J.; Chao, P.; Jin, X.; Li, W. Dynamic equivalent modeling of direct-drive PMSG wind farms based on the transient active power response characteristics. In Proceedings of the 2016 IEEE 8th International Power Electronics and Motion Control Conference (IPEMC-ECCE Asia), Hefei, China, 22–26 May 2016; pp. 2925–2930.
10. Fernández, L.; García, C.; Saenz, J.; Jurado, F. Equivalent models of wind farms by using aggregated wind turbines and equivalent winds. *Energy Convers. Manag.* **2009**, *50*, 691–704. [CrossRef]
11. Meng, Z.J.; Xue, F. An Investigation of the Equivalent Wind Method for the Aggregation of DFIG Wind Turbines. In Proceedings of the 2010 Asia-Pacific Power and Energy Engineering Conference, Chengdu, China, 28–31 March 2010; pp. 1–6. [CrossRef]
12. Erlich, I.; Kretschmann, J. Modeling of wind turbines based on doubly-fed-induction generators for power system stability sdudies. *IEEE Trans. Power Syst.* **2007**, *22*, 909–919. [CrossRef]
13. Banakar, H.; Ooi, B.T. Clustering of Wind Farms and its Sizing Impact. *IEEE Trans. Energy Convers.* **2009**, *24*, 935–942. [CrossRef]
14. Baohui, Z.; Guanghui, L. The impact of wind power integration on relay protection (II)—Research on electromagnetic transient equivalent modeling of doubly-fed wind farms. *Electr. Power Autom. Equip.* **2013**, *33*, 1–7.
15. Shafiu, A.; Anaya-Lara, O.; Bathurst, G.; Jenkins, N. Aggregated Wind Turbine Models for Power System Dynamic Studies. *Wind. Eng.* **2006**, *30*, 171–185. [CrossRef]
16. Guixiong, H.; Qin, H. Research on aggregation of dynamic equivalent parameters of constant speed generators in wind farms. *Renew. Energy Resour.* **2009**, *27*, 14–18.

17. Zhenghang, H.; Chao, Q. Influence of simplified converter model of doubly-fed wind turbine on simulation results. *Electr. Technol.* **2011**, *09*, 60–64.
18. Jing, L.; Wei, W. Simplified dynamic model of doubly-fed induction generator and its application in wind power. *Electr. Power Autom. Equip.* **2015**, *25*, 58–62.
19. Pupu, C.; Weixing, L. An Active Power Response Based Practical Equivalent Method for DFIG Wind Farms. *Proc. CSEE* **2018**, *6*, 1639–1646.
20. Van, T.L.; Nguyen, T.H.; Lee, D.-C. Advanced Pitch Angle Control Based on Fuzzy Logic for Variable-Speed Wind Turbine Systems. *IEEE Trans. Power Electron.* **2015**, *30*, 578–587. [CrossRef]
21. Kim, H.W.; Kim, S.S. Modeling and control of PMSG-based variable-speed wind turbine. *Electr. Power Syst. Res.* **2010**, *80*, 46–52. [CrossRef]
22. Alizadeh, M.; Kojori, S.S. Augmenting effectiveness of control loops of a PMSG (permanent magnet synchronous generator) based wind energy conversion system by a virtually adaptive PI (proportional integral) controller. *Energy* **2015**, *91*, 610–629. [CrossRef]
23. Li, S.; Haskew, T.A.; Xu, L. Conventional and novel control designs for direct driven PMSG wind turbines. *Electr. Power Syst. Res.* **2010**, *80*, 328–338. [CrossRef]
24. Muljadi, E.; Butterfield, C.; Ellis, A.; Mechenbier, J.; Hochheimer, J.; Young, R.; Miller, N.; Delmerico, R.; Zavadil, R.; Smith, J. Equivalencing the collector system of a large wind power plant. In Proceedings of the 2006 IEEE Power Engineering Society General Meeting, Montreal, QC, Canada, 18–22 June 2006.
25. Mohsen, R.; Mostafa, P. Dynamic behavior analysis of doubly-fed induction generator wind turbines-the influence of rotor and speed controller parameters. *Electr. Power Energy Syst.* **2010**, *32*, 464–477.